Spin-density waves in heavy-fermion compounds: A theoretical study

Zs. Gulácsi and M. Gulácsi
Institute of Isotopic and Molecular Technology, 3400-Cluj-5, P.O. Box 700, Romania
(Received 2 April 1986; revised manuscript received 29 December 1986)

The first theoretical description of the itinerant antiferromagnetic state in heavy-fermion systems is presented in detail. We analyze the phase diagram, the stability of the phases, the magnetic susceptibility, and the specific heat. For the case in which the gap vanishes in points on the Fermi surface, the deduced results are in good agreement with the experimental data.

I. INTRODUCTION

During the last few years a great deal of experimental and theoretical works[1] have been devoted to understanding the properties of the heavy-fermion compounds. The theoretical analyses published up to now[2] have focused on descriptions of the Kondo lattice and the superconducting properties of these systems. However, recent experimental data[3] emphasize the magnetically ordered ground state in some heavy-fermion systems. Among these, we must mention the U_2Zn_{17},[4] UCd_{11},[5] and $NpBe_{13}$ (Ref. 6) compounds, for which, at low temperature, itinerant antiferromagnetic properties are claimed.[3-6] There are other compounds in which the magnetically ordered ground state is presumed to exist in some temperature domain, such as $U_{1-x}Th_xBe_{13}$,[7] URu_2Si_2,[8] UCu_5,[9] $CePb_3$,[10] but this is an experimental field that is developing so rapidly that until now, few relevant conclusions have been produced. These previously presented experimental data need theoretical descriptions which should analyze the magnetic properties of the heavy-fermion ground state.

For the antiferromagnetic characteristics of U_2Zn_{17}, UCd_{11}, and $NpBe_{13}$ compounds the experimental data strongly indicates an itinerant origin. The magnetic susceptibility (χ) and the specific heat (C_p) plots for these systems; the ordered moment of some tenths of μ_B which is considerably smaller than the Curie-Weiss effective localized moment;[3] the recent neutron diffraction data;[11] and the fact that the magnetic properties are strongly affected by substitutions on sites, completely unlike usual local-moment behavior (like Zn in U_2Zn_{17}),[3] support this observation. In order to obtain theoretically such properties, usually a spin-density-wave (SDW) formation is claimed. Starting from this idea, we analyze, in this paper the possibilities of SDW formation in heavy-fermion systems. We stick to this phase, and so we will neglect (as the models which analyze the superconducting properties[2,12]) other condensed phases. The analysis is conducted in such a way that the study of the coexistence between the SDW and the superconducting ground states (which seems to be experimentally proved[3,7]) becomes possible. (In fact, this study is underway.) In this paper we concentrate upon the possible descriptions of the SDW state in heavy-fermion systems, together with their characteristics and properties. Some preliminary conclusions were presented in two short papers.[13] This article contains the detailed prescription of the theoretical results concerning a simple crystal structure.

The paper is organized as follows. In Sec. II we describe the Hamiltonian and after a discussion concerning the nesting properties, we deduce the Green's functions. The characteristic physical quantities and the phase diagram are described in Secs. III and IV. A comprehensive analysis of different SDW phases is given in Sec. V. Section VI is dedicated to discussions and conclusions.

II. MODEL

The experimentally measured[4-6] specific-heat jump at the Néel temperature (T_N) is comparable in magnitude with the normal specific heat C_n at $T \rightarrow T_N$. Thus, we consider that the same f electrons which are responsible for the heavy-fermion properties give rise to the SDW phase too. Furthermore, the above presented experimental data show that the itinerant antiferromagnetic ground state which is realized in a large domain of the phase diagram (PD) substantially differs from the classical Overhauser-type[14] or Fedders-Martin–type[15] phase: C_p well below T_N behaves like T^3,[4-6] the gap in certain crystallographic directions must still be zero at $T=0$,[16,17] and the SDW state appears only when the f electrons, which in the high-temperature domain are localized on the rare-earth or actinide sites, become coherent and form a heavy-fermion band.[1-3] In these circumstances, we start our considerations with a Hamiltonian which describes such a band and has the form[18]

$$H_1 = -\tfrac{1}{2}\sum_{i,j,\sigma}(t a^{\dagger}_{i,\sigma}a_{j,\sigma} + \text{H.c.}) + \tfrac{1}{2}\sum_{i,\sigma} U a^{\dagger}_{i,\sigma}a_{i,\sigma}a^{\dagger}_{i,-\sigma}a_{i,-\sigma} \ . \quad (1)$$

The microscopic origin of H_1 arises from a simple description of the Kondo-lattice system.[18,19] The first term describes a narrow half-filled band, which gives rise to the $\varepsilon_k = -t\gamma_k$ dispersion relation in k space. $t = 2T_K/\pi z$, where T_K is the Kondo temperature and z is the number of the nearest-neighbor sites denoted by i and j. The second term is the renormalized one site repulsion. In the case of heavy-fermionic systems, it is known[2] that the concrete band structure plays an important role. Because of this, in this paper we analyze a cubic system, where $\gamma_k = 2[\cos(ak_x)+\cos(ak_y)+\cos(ak_z)]$ with a as

lattice constant. The results however, can be easily generalized to other symmetry species.[13,20]

Furthermore, the electron-electron interactions appear to dominate the behavior of the analyzed systems at low temperatures.[1,3,4] So, in order to describe an SDW state, besides H_1 we must take into account these interactions in a way which emphasizes the difference between the contributions which arise from different spin configurations on nearest-neighbor sites. For this reason we consider spin-dependent interactions between the nearest-neighbor sites in the following Hamiltonian term:

$$H_2=\tfrac{1}{2}\sum_{i,j,\sigma} V a^{\dagger}_{i,\sigma}a_{i,\sigma}a^{\dagger}_{j,\sigma}a_{j,\sigma}-\tfrac{1}{2}\sum_{i,j,\sigma} I a^{\dagger}_{i,\sigma}a_{j,-\sigma}a^{\dagger}_{i,-\sigma}a_{j,\sigma} -\tfrac{1}{2}\sum_{i,j,\sigma} J a^{\dagger}_{i,\sigma}a_{i,\sigma}a^{\dagger}_{j,-\sigma}a_{j,-\sigma} \ . \tag{2}$$

Because the phononic terms are considered separately, we consider that the terms from H_2 have a different nonphononic origin, for a discussion of this see Ref. 13. Our study shows that these terms are those which greatly contribute to an SDW state description in the analyzed systems. We have to mention that the last term was already successfully used in the explanation of the $1/T_1$ relaxation rate in heavy-fermion superconductors,[22] while V and J were tested[21] some years ago in an analysis of the itinerant antiferromagnetic properties. These two terms arise from a standard $(\lambda_1\delta_{\alpha\beta}\delta_{\gamma\delta}+\lambda_2\sigma_{\alpha\beta}\cdot\sigma_{\gamma\delta})$-like exchange term between the nearest-neighbor sites, where $\delta_{\alpha\beta}$ and $\sigma_{\alpha\beta}$ are the Kronecker symbol and the Pauli matrices, respectively. The second term in H_2 tries to model the fluctuation effects in a simple manner. As will be seen later (see Sec. IV), the introduction of I is necessary if we want to obtain energetically stable odd k-dependent gap functions.

As we have mentioned before, the phononic terms are taken into account separately, by the following Hamiltonian term[19]

$$H_3=-\tfrac{1}{2}\sum_{i,j,\sigma,\sigma'}\tilde{g}_1 a^{\dagger}_{i,\sigma}a_{j,\sigma}a^{\dagger}_{j,\sigma'}a_{i,\sigma'} -\tfrac{1}{2}\sum_{i,j,\sigma,\sigma'}\tilde{g}_2 a^{\dagger}_{i,\sigma}a_{i,\sigma}a^{\dagger}_{j,\sigma'}a_{j,\sigma'} -\tfrac{1}{2}\sum_{i,j,\sigma}\tilde{g}_3 a^{\dagger}_{i,\sigma}a_{i,\sigma}(a^{\dagger}_{i,-\sigma}a_{j,-\sigma}+\text{H.c.}) \ . \tag{3}$$

As expected[1,3] the contributions from H_3 will not play an essential role in a SDW phase description [see Eq. (17): the expressions of the effective coupling constants are only renormalized by $\tilde{g}_i$]. However, H_3 is important in the analysis of the superconducting properties. For this reason and taking into account the future developments which need a study of the existence of the SDW and the superconducting phase, the Hamiltonian we use is $H_1+H_2+H_3$.

In order to describe an SDW phase, we must analyze the nesting properties at first. In our case, being a cubic system, a Q vector oriented along the [111] direction in k space,

$$\mathbf{Q}_{111}=(\pi/a)(\hat{\mathbf{i}}+\hat{\mathbf{j}}+\hat{\mathbf{k}}) \ , \tag{4}$$

produces the required nesting

$$\varepsilon_{k+Q}=-\varepsilon_k \ , \tag{5}$$

without which the SDW state cannot be formed.[15] Nesting conditions can be obtained for other crystal structures too, so that, the presented description could be with no difficulty given for other symmetry species[13] too. We must mention that we have a commensurate spin-density wave [see Eq. (4)] as the neutron diffraction measurements suggest.[11]

Furthermore, we introduce the following average:

$$\tau^{\pm\sigma}(k)=\langle a^{\dagger}_{k,\pm\sigma}a_{k+Q,\pm\sigma}\rangle \ , \tag{6}$$

where Q is fixed at the Q_{111} value. The effective Hamiltonian which can be obtained, in this way becomes

$$H_{\text{eff}}=\frac{1}{N}\sum_{k,\sigma}\varepsilon_k a^{\dagger}_{k,\sigma}a_{k,\sigma}+\tfrac{1}{2}\frac{1}{N}\sum_{k,k',\sigma}\{a^{\dagger}_{k,\sigma}a_{k+Q,\sigma}[g_1^{-}(k,k')\tau^{+\sigma}(k')+g_2^{-}(k,k')\tau^{-\sigma}(k')]+\text{H.c.}\} \ . \tag{7}$$

We use the notations

$$\begin{aligned} g_1^{\pm}(k,k')&=(\tilde{g}_2-\tilde{g}_1-V)[6\pm\gamma(k-k')] \ , \\ g_2^{\pm}(k,k')&=U+6(\tilde{g}_2+J)\mp I\gamma(k+k')\mp\tilde{g}_1\gamma(k-k') \ . \end{aligned} \tag{8}$$

In our analysis we are interested in the following Green's functions:

$$\begin{aligned} G^{\sigma}(k,i\omega_n)&=\langle\langle a_{k,\sigma}\mid a^{\dagger}_{k,\sigma}\rangle\rangle_{i\omega_n} \ , \\ F^{\sigma}(k,i\omega_n)&=\langle\langle a_{k+Q,\sigma}\mid a^{\dagger}_{k,\sigma}\rangle\rangle_{i\omega_n} \ , \end{aligned} \tag{9}$$

where $G^{\sigma}(k,i\omega_n)$ is the normal and $F^{\sigma}(k,i,\omega_n)$ is the anomalous Green's function. Using standard methods, from H_{eff} one obtains

$$\begin{aligned} G^{\sigma}(k,i\omega_n)&=(i\omega_n+\varepsilon_k)/N_{\sigma} \ , \\ F^{\sigma}(k,i\omega_n)&=g^{*}_{\sigma}(k)/N_{\sigma} \ , \end{aligned} \tag{10}$$

where

$$\begin{aligned} N_{\sigma}&=(i\omega_n)^2-\varepsilon_k^2-\mid g_{\sigma}(k)\mid^2 \ , \\ g^{*}_{\sigma}(k)&=\frac{1}{N}\sum_{k'}[g_1^{+}(k,k')\tau^{+\sigma}(k')+g_2^{+}(k,k')\tau^{-\sigma}(k')] \ ; \\ g^{*}_{-\sigma}(k)&=-g^{*}_{\sigma}(k) \ . \end{aligned} \tag{11}$$

The knowledge of the Green's functions makes it possible to express the SDW gap and some physical quantities of interest. This will be done in the following section.

III. CHARACTERISTIC QUANTITIES

The SDW gap can be given in the following way

$$\Delta_S(k)=\frac{\beta^{-1}}{2}\frac{1}{N}\sum_{k',n} g_S(k,k')\text{Tr}_{\sigma}\sigma^z F^{\sigma}(k',i\omega_n) \ , \tag{12}$$

where $g_S(k,k')=g_1^+(k,k')-g_2^+(k,k')$. Using Eqs. (10)–(12) the expression of $\Delta_S(k)$ becomes

$$\Delta_S(k)=\frac{\beta^{-1}}{2}\frac{1}{N}\sum_{k',n}\frac{g_S(k,k')\Delta_S(k')}{(i\omega_n)^2-\varepsilon_{k'}^2-|\Delta_S(k')|^2} . \quad (13)$$

The structure of $g_S(k,k')$ imposes the following expression for $\Delta_S(k)$

$$\Delta_S(k)=\sum_{i=0}^{6} S_i(k)\Delta_i . \quad (14)$$

For the symmetry-adapted functions $S_i(k)$, we have

$$\begin{aligned} &S_0(k)=1 , \\ &S_1(k)=\gamma_k , \\ &S_2(k)=\sqrt{6}[\cos(ak_x)-\cos(ak_y)] , \\ &S_3(k)=\sqrt{2}[\cos(ak_x)+\cos(ak_y)-2\cos(ak_z)] , \\ &S_4(k)=\sin(ak_x) , \\ &S_5(k)=\sin(ak_y) , \\ &S_6(k)=\sin(ak_z) , \end{aligned} \quad (15)$$

where $S_i(k)$ are orthogonal functions, each being along a fixed irreducible representation Γ_i of the cubic group O_h. For $i=0,1$, $\Gamma_i=A_{1g}$, for $i=2,3$, $\Gamma_i=E_g$, and for $i=4,5,6$, $\Gamma_i=F_{1u}$.[13,19,20] The odd-parity gap functions will be denoted with $\tilde{\Delta}_4=\Delta_x\sin k_x+\Delta_y\sin k_y+\Delta_z\sin k_z$, where $\Delta_4=\Delta_x$, $\Delta_5=\Delta_y$, and $\Delta_6=\Delta_z$. In this way Eq. (13) is reduced to

$$\Delta_i=\frac{1}{N}\sum_k g_i S_i(k)\frac{\Delta_S(k)}{2E(k)}\tanh\left[\frac{\beta E(k)}{2}\right] ; \quad i=0\text{–}6 . \quad (16)$$

We have $E(k)=(\varepsilon_k^2+|\Delta_S(k)|^2)^{1/2}$ and the effective coupling constants which are renormalized by the phononic contributions, are

$$\begin{aligned} &g_0=U+6(V+J+\tilde{g}_1) , \\ &g_1=g_2=g_3=(V-I-\tilde{g}_2)/6 , \\ &g_4=g_5=g_6=2(V+I-\tilde{g}_2) . \end{aligned} \quad (17)$$

Whenever necessary, we will use the notation $\tilde{V}=V-\tilde{g}_2$.

The presented model can be considered as an extension of the description given by Miyake *et al.*[19] for the case in which the exchange interactions and the phononic contributions are equally important. The existence of the effective coupling constants g_0, g_2, and g_4 (such effective constants can be obtained in the superconducting case too) emphasizes that the competition between the same interactions gives rise to superconductivity or itinerant magnetic properties in heavy-fermion systems and in the two cases above mentioned, only the strength of the contributing interactions is different (see for example Ott *et al.*[4]). However, we must mention that the gap equation in the superconducting case differs significantly from Eqs. (14)–(17). This is due to the γ_k term in the first, and the $2g_3$ term in the second gap, Eq. (31) of Ref. 19, because the even k solutions and the whole PD are totally different in that case.

The order parameter for the SDW phase [see Eqs. (14) and (15)] is strongly k dependent. While Δ_0 resembles the classical gap,[14,15] the Δ_i, $i\geq 1$ contributions describe SDW states which differ from the Overhauser-type[14] or Fedders-Martin-type[15] phases, in agreement with the experimental[16] observation that the gap vanishes in some crystallographic directions. A consequence of this is the unusual temperature dependence of the physical quantities, which describe the heavy fermion systems and cannot be deduced from the classical models.

In order to be realistic in the construction of the PD, we have to make the energetical stability analysis, too. The free energy of the system can be deduced following Leggett.[24] After some algebra, its expression becomes

$$F=F_0+\sum_{i=0}^{6}\frac{|\Delta_i|^2}{g_i}-\frac{1}{N}\sum_k \ln\frac{\cosh\frac{\beta E(k)}{2}}{\cosh\frac{\beta\varepsilon_k}{2}} , \quad (18)$$

where F_0 is the free energy of the paramagnetic state (all $\Delta_i=0$). We are also interested in the deduction of some experimentally measured physical quantities. Thus, we will calculate the specific heat $C_p(T)$ and the magnetic susceptibility $\chi(T)$. The expression of $C_p(T)$ can be easily obtained from the entropy[24]

$$C_p(T)=\frac{\beta^2}{2}\frac{1}{N}\sum_k E(k)\left[E(k)+\beta\frac{dE(k)}{d\beta}\right]\cosh^{-2}\frac{\beta E(k)}{2} . \quad (19)$$

The magnetic susceptibility is obtained by means of the linear response theory. The magnetic susceptibility tensor χ_{ij}, which describes the response of the total induced spin magnetization in the direction i, under the perturbation of an uniform static magnetic field in the direction j is expressed as

$$\chi_{ij}=\chi_1\delta_{ij}+\chi_2(\delta_{ki}\delta_{kj}-\epsilon_{ikl}\epsilon_{lkj}) , \quad (20)$$

where δ_{ij} is the Kronecker symbol and ϵ_{ijk} is the antisymmetrical tensor defined as

$$\sigma^i_{\alpha\beta}\sigma^k_{\beta\gamma}=\delta_{ij}\delta_{\alpha\gamma}+i\epsilon_{ikl}\sigma^l_{\alpha\gamma} , \quad (21)$$

$\sigma^j_{\alpha\beta}$ being the Pauli matrices. χ_1 and χ_2 are expressed as

$$\begin{aligned} \chi_1(T)&=-2\mu_B^2\beta^{-1}\frac{1}{N}\sum_{k,n}G^\sigma(k,i\omega_n)G^\sigma(k,i\omega_n) , \\ \chi_2(T)&=-2\mu_B^2\beta^{-1}\frac{1}{N}\sum_{k,n}F^\sigma(k,i\omega_n)F^\sigma(k,i\omega_n) , \end{aligned} \quad (22)$$

where μ_B is the Bohr magneton. The total magnetic susceptibility becomes

$$\chi(T)=\tfrac{1}{3}[\chi_1(T)+\chi_2(T)]+\tfrac{2}{3}[\chi_i(T)-\chi_2(T)] . \quad (23)$$

From Eqs. (10) and (20)–(23) one obtains

$$\chi(T)=\mu_B^2[\tfrac{1}{3}Y(T)+\tfrac{2}{3}Z(T)] , \quad (24)$$

where

$$Y(T)=\frac{\beta}{2}\frac{1}{N}\sum_k \cosh^2\frac{\beta E(k)}{2} \tag{25}$$

and

$$Z(T)=\frac{1}{N}\sum_k \frac{\partial}{\partial\epsilon_k}\left[\frac{\epsilon_k}{E(k)}\tanh\frac{\beta E(k)}{2}\right]. \tag{26}$$

IV. PHASE DIAGRAM

Concerning the phase diagram (PD), the results were obtained by using simultaneously the gap equations, Eq. (16) and the free energy expression, Eq. (18) in order to obtain energetically stable phases. Figure 1 presents the results obtained for $T=0$. As Eq. (17) reflects we have three global coupling constants which characterize the model: g_0, g_2, and g_4. Depending on these, the PD will be as in Fig. 1(d). As can be seen, we have only three energetically stable phases; Δ_0, $\tilde{\Delta}_4$, and Δ_2, Δ_3 (for the last phase the Δ_2 and Δ_3 order parameters coexist). The solid curves in Figs. 1(a), 1(b), and 1(c) represent phase separation lines of PD in the $g_4=0$, $g_2=0$, and $g_0=0$ planes, respectively. The Δ_2, Δ_3 coexistence is a regular one, because these two order parameters have the same symmetry (E_g). Among these we have regular coexistence between the Δ_0 and Δ_1 phases (both A_{1g}) in the region situated between the (3) dashed line and the g_2 axis [Fig. 1(a)], but this is unstable, because it has greater free energy than the Δ_2, Δ_3 phase

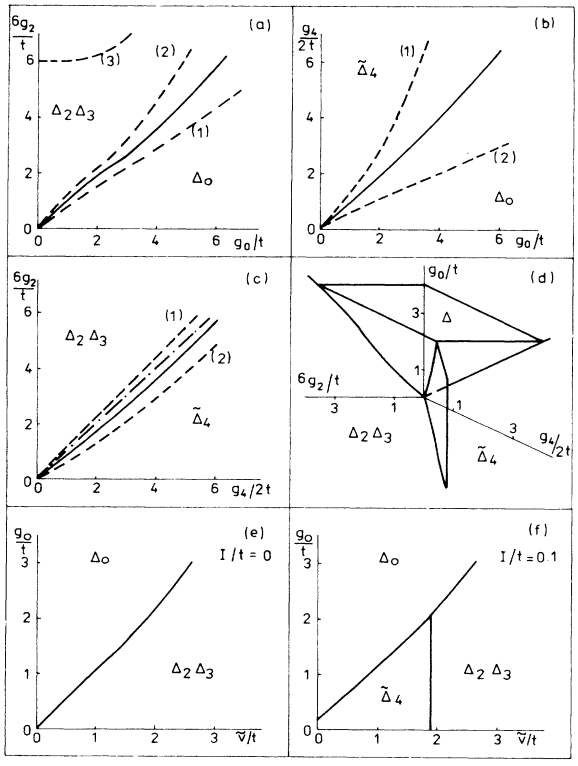

FIG. 1. Phase diagram of the system at $T=0$. (a) The $g_4=0$ plane; (b) the $g_2=0$ plane; (c) the $g_0=0$ plane; (d) the global phase diagram in the $(g_0/t,g_2/t,g_4/t)$ space; (e) the $(g_0/t,\tilde{V}/t)$ plane for $I/t=0$; (f) the $(g_0/t,\tilde{V}/t)$ plane for $I/t=0.1$. The dashed lines delimitate unstable domains (see text).

Between the dashed curves (1) and (2) in Figs. 1(a), 1(b), and 1(c) we have irregular coexistence between gaps with different symmetries: $\Delta_0\neq0$, $\Delta_2\neq0$, $\Delta_3\neq0$ in Fig. 1(a); $\Delta_0\neq0$, $\tilde{\Delta}_4\neq0$ in Fig. 1(b), and $\tilde{\Delta}_4\neq0$, $\Delta_2\neq0$, $\Delta_3\neq0$ in Fig. 1(c), respectively. These solutions are allowed by the gap equations, but they are energetically unstable. For example, at the dashed line (2) [Fig. 1(a)] the Δ_2, Δ_3 phase appears within a Δ_0 state. The new phase $\Delta_0\neq0$, $\Delta_2\neq0$, $\Delta_3\neq0$ situated below the (2) curve has lower energy than the $\Delta_0\neq0$ phase, but greater energy than the $\Delta_2\neq0$, $\Delta_3\neq0$, $\Delta_0=0$ phase, which can exist in the same region of the PD. Similar results can be obtained for other irregular coexistences, too. This conclusion shows that, because of the differences in the symmetry of the $S_i(k)$ functions, the coexistence between different Δ_i terms cannot appear unrestricted. This is in good agreement with the results of Balian and Werthamer[25] concerning the coexistence of different symmetry species.

The $\tilde{\Delta}_4$ phase can be also considered as a regular coexistence state, but we treat it as a single vector solution with components Δ_x, Δ_y, Δ_z. The existence of this phase is strongly connected to the I value. To show this, we mention that in Fig. 1(c) the dot-dashed curve represents

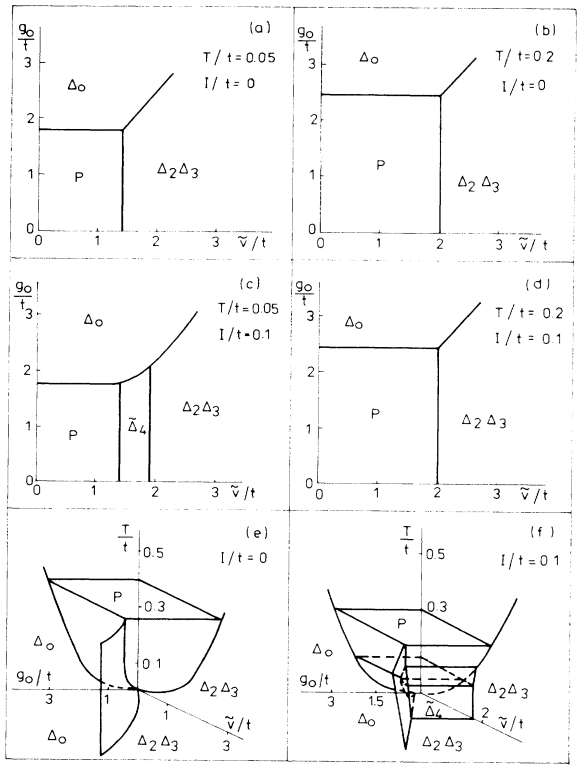

FIG. 2. Phase diagram of the system at $T\neq0$. (a) The $(g_0/t,\tilde{V}/t)$ plane for $T/t=0.05$ and $I/t=0$; (b) the plane $(g_0/t,\tilde{V}/t)$ for $T/t=0.2$ and $I/t=0$; (c) the $(g_0/t,\tilde{V}/t)$ plane for $T/t=0.05$ and $I/t=0.1$; (d) the $(g_0/t,\tilde{V}/t)$ plane for $T/t=0.2$ and $I/t=0.1$; (e) the global phase diagram in the $(g_0/t,\tilde{V}/t,T/t)$ space for $I/t=0$; (f) the global phase diagram in the $(g_{0/t},\tilde{V}/t,T/t)$ space for $I/t=0.1$.

the $\tilde{V}-I=\tilde{V}+I$ line. Because the separation between the $\tilde{\Delta}_4$ and the Δ_2, Δ_3 phases [the solid line in Fig. 1(c)] is situated below this curve, for $I=0$ the $\tilde{\Delta}_4$ phase cannot appear [Fig. 1(e)]. If $I\neq 0$, the shape of the PD is automatically modified [Fig. 1(f)]. All the other solutions of Eq. (16), (e.g., $\Delta_1\neq 0$, $\Delta_2\neq 0$, $\Delta_3=0$; $\Delta_2=0$, $\Delta_3\neq 0$; or the other nonmentioned coexistence states) have greater energy than the stable phases of PD.

In Figs. 2(a)–2(f) we show the PD for $T\neq 0$. The space used is $(g_0/t,\ \tilde{V}/t,\ T/t)$ and I/t is a parameter. For $I/t=0$, we obtain the PD from Fig. 2(e). The $T=0$ section of this figure is given in Fig. 1(e) and other two $T/t=$const planes are presented in Figs. 2(a) and 2(b). The paramagnetic phase is denoted by P. As one can see, we do not have a $\tilde{\Delta}_4$ phase in this case.

For $I/t=0.1$, the PD is given in Fig. 2(f). The $T/t=0$, 0.05, and 0.2 sections are given in Figs. 1(f), 2(c), and 2(d), respectively. The phase transition from the P to the ordered phases are of the second kind. It must be mentioned that the $\tilde{\Delta}_4$ and the Δ_2, Δ_3 phases can be generated by many solutions of Eq. (16). From these, in the construction of the PD we have used the one which gives the minimum possible free energy value (see Sec. V).

The Δ_0 phase (since its gap does not present k dependence) resembles Overhauser-type[14] or Fedders-Martin-type[15] SDW state. However, in our case, two new energetically stable SDW phases appear, with gaps which vanish for certain k directions (as the experimental results suggested[16,17]). Under these circumstances, a description of the magnetic ground state of heavy fermions becomes possible, and it is made in the next section.

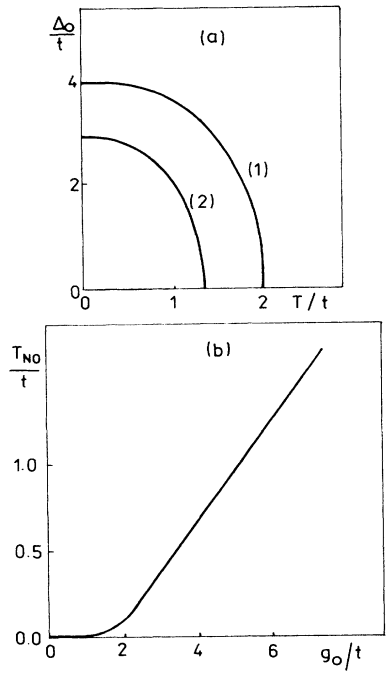

FIG. 3. Characteristics of the Δ_0 phase. (a) The reduced gap Δ_0/t as a function of the reduced temperature T/t for $g_0/t=9$ curve (1) and $g_0/t=6.3$ curve (2); (b) the critical temperature vs the coupling constant g_0.

V. ANALYSIS OF DIFFERENT SDW PHASES

In this section we analyze (separately) the three stable SDW phases of the PD. Still, we have to underline that the k sum is performed using $N^{-1/3}\sum_{k_i}\rightarrow(a/2\pi)\int_{-\pi/a}^{+\pi/a}dk_i$, $i=x,y,z$ and all the integrals which appear in this section, denoted by I_1^0, I_2^0, $I_1^{2/3}$, . . . , are given in the Appendix.

A. Δ_0 phase

The characteristic gap equation for this phase is obtained from Eq. (16) for $i=0$, and $\Delta_i=0$ for all $i\geq 1$. The precise numerical result concerning the temperature dependence of the gap and the critical temperature T_{Ni}/t (in this case $i=0$) as a function of the coupling constant g_0, is given in Fig. 3(a) and 3(b), respectively. The analytical expression of $\Delta_0(T)$ at $T\rightarrow 0$ is

$$\Delta_0(T)=\Delta_0(T=0)-g_0T^{3/2}I_1^0e^{-\Delta_0(T=0)/T}\ , \tag{27}$$

and can be found by making the following change of the integral variables: $x_1=\sqrt{\beta}\cos(\pi x)$, $x_2=\sqrt{\beta}\cos(\pi y)$, and $x_3=\sqrt{\beta}\cos(\pi x)$. The $\Delta_0(T=0)/T_{N0}$ fraction is constant, i.e., approximately equal to 2, for $g_0/t>2$. If we are situated at a temperature range $T\lesssim T_{N0}$, the gap becomes

$$\Delta_0=t[k_0I_0^0(T_{N0},1/\sqrt{2})]^{-1/2}(1-T/T_{N0})^{1/2}\ , \tag{28}$$

where

$$\begin{aligned} &k_0=3.50t/T_{N0},\quad \text{for } t/T\gg 1\ ,\\ &k_0=2.62,\quad \text{for } t/T\sim 1\ ,\\ &k_0=2,\quad \text{for } t/T\ll 1\ . \end{aligned} \tag{29}$$

The expressions for the Néel temperature are

$$\begin{aligned} &T_{N0}=t\exp[-t/(0.14g_0)],\quad \text{for } t/T\gg 1\ ,\\ &T_{N0}=0.19g_0,\quad \text{for } t/T\sim 1\ ,\\ &T_{N0}=g_0/4,\quad \text{for } t/T\ll 1\ . \end{aligned} \tag{30}$$

The $C_p(T)$ expression can be derived from Eq. (19). For $T\rightarrow 0$, $\partial E(k)/\partial\beta$ bring a negligible contribution. For the first term we use the same integral variable transformation as for Eq. (27), and we obtain

$$C_p(T)=2T^{-1/2}\Delta_0^2(T=0)e^{-\Delta_0(T=0)/T}[I_1^0+O(T)]\ . \tag{31}$$

As to the magnetic susceptibility, first of all we have to emphasize some general properties of Eqs. (24)–(26) which are true for every i state. For $T\rightarrow T_{Ni}$, we have

$$Y(T_{Ni})=Z(T_{Ni})=\chi(T_{Ni})/\mu_B^2\ . \tag{32}$$

In the case of classical SDW, Eq. (32) gives the temperature independent Pauli susceptibility $\chi_P(T)=2N(0)\mu_B^2$. From Eq. (32) the paramagnetic susceptibility can be reobtained, for $T>T_{Ni}$ and $T\rightarrow T_{Ni}$, by putting $\Delta_i=0$. However, in this case $\chi_P(T)$ has a meaning just above

T_{Ni}, because at higher temperatures the system undergoes a local moment regime. We have to mention that an exact numerical result shows that $\chi_P(T)$ is nearly constant in a relatively large T/t domain, i.e., $t\chi_P/\mu_B^2 \simeq 0.28$ for $T/t \in [0.05,0.7]$. For a greater T/t it decreases, so that, for example at $T/t=5$, $t\chi_P/\mu_B^2$ is 0.094.

For $T\to 0$, at any i, $Z(T)$ becomes a temperature-independent constant $Z(0)$ and the T dependence of $\chi(T)$ is determined by $Y(T)$. For the classical SDW, a similar situation is obtained with $Z(0)=1$. For the Δ_0 phase, in the $T\to 0$ limit we obtain

$$\chi(T)=\mu_B^2\left[\tfrac{2}{3}Z(0)+\frac{T^2}{3}I_2^0\right] . \tag{33}$$

To obtain Eq. (33) an integral representation of $\cosh^{-2}x$ was taken into account, which introduces the x_4 integral variable (see the Appendix), after which the same integral variable transformation was used as for I_1^0. As it can be seen, one obtains exponential dependence for $C_p(T)$ and T^2 behavior for $\chi(T)$ in the $T\to 0$ limit; thus, the Δ_0 phase resembles classical SDW state.[14,15] However, experimental measurements[3,4] show a T^2 behavior in $\chi(T)$ and give a T^3 dependence in $C_p(T)$ for $T\to 0$. Thus, probably it is not the Δ_0 phase which is realized in the measured heavy-fermion systems.

B. Δ_2, Δ_3 phase

The gap equations which we must analyze in this case can be obtained from Eq. (16) for $i=2,3$ with $\Delta_0=\Delta_1=\tilde{\Delta}_4=0$. The two coupled integral equations which result allow simple solutions like $\Delta_2\neq 0$, $\Delta_3=0$ and $\Delta_2=0$, $\Delta_3\neq 0$, but these have greater free energy than the coexistence phase. Thus, only the $\Delta_2\neq 0$, $\Delta_3\neq 0$ phase will be analyzed below. All such solutions have the same critical temperature T_{N2} [Fig. 4(a)], and they can be real or complex variables. From these, the minimum possible free energy has the $\Delta_2=\Delta$, $\Delta_3=\pm i\Delta$ (or equivalent) solution, which was used in the construction of the PD. In Fig. 4(b) we present some exact numerical results concerning the Δ versus T variations at fixed g_2/t values.

The analytical expression of $\Delta(T)$ in the $T\to 0$ limit can be given as

$$\Delta(T)=\Delta(T=0)-\tfrac{1}{2}g_2T^4\Delta(T=0)I_{c1}^{2,3} . \tag{34}$$

Equation (34) is found by expanding the tanh$x$ functions and by changing the integral variables in $x_1=\beta\cos(\pi x)$, $x_2=\beta\cos(\pi y)$, and $x_3=\beta\cos(\pi z)$. The analytical approximations for T_{N2} are the following

$$\begin{aligned} &T_{N2}=t\exp[-t/(1.07g_2)] \quad \text{for } t/T\gg 1 ,\\ &T_{N2}=1.25g_2 \quad \text{for } t/T\sim 1 ,\\ &T_{N2}=3g_2/2 \quad \text{for } t/T\ll 1 . \end{aligned} \tag{35}$$

The $T_{N2}/\Delta(T=0)$ ratio slowly decreases with g_2/t, so that it becomes 2.5 and 2.08 at $6g_2/t=2$ and 8, respectively. In the vicinity of T_{N2}, Δ can be expressed as

$$\Delta=t\,[k_{2c}I_0^0(T_{N2},(S_2^2+S_3^2)/\sqrt{2})]^{-1/2}(1-T/T_{N2})^{1/2} , \tag{36}$$

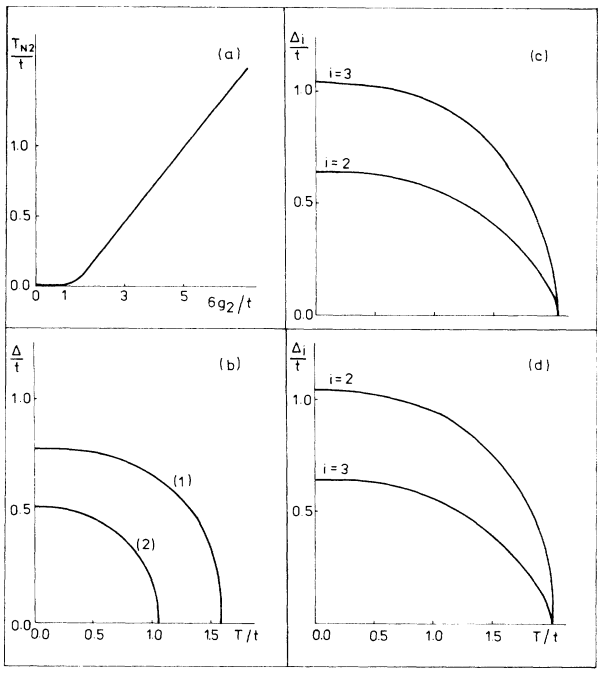

FIG. 4. Characteristics of the Δ_2, Δ_3 phase. (a) The critical temperature vs the coupling constant g_2; (b) the reduced gap Δ/t as a function of the reduced temperature T/t for $g_2/t=1.16$, curve (1) and $g_2/t=0.83$, curve (2) in the case of the complex solution; the reduced gaps Δ_2/t and Δ_3/t as a function of the reduced temperature T/t are presented in (c) and (d), respectively, for $g_2/t=1.41$, in the case of the real symmetrical solution.

where

$$\begin{aligned} &k_{2c}=0.23t/T_{N2} \quad \text{for } t/T\gg 1 ,\\ &k_{2c}=0.20 \quad \text{for } t/T\sim 1 ,\\ &k_{2c}=\tfrac{1}{6} \quad \text{for } t/T\ll 1 . \end{aligned} \tag{37}$$

with S_2 and S_3 given in Eq. (15). The specific heat can be obtained just as in the previous paragraph. Starting from Eq. (19) and using the same integral variable transformation as for Eq. (34), in the $T\to 0$ limit one obtains

$$C_p(T)=\frac{T^3}{2}I_{c2}^{2,3} . \tag{38}$$

As we mentioned in Sec. V A, for the magnetic susceptibility in the $T\to 0$ limit, we must consider only the $Y(T)$ term [see Eq. (25)], because the $Z(T)$ term brings a constant contribution $Z(0)$. With the same technique as for the specific heat, we find

$$Y(T)=T^2I_{c3}^{2,3} . \tag{39}$$

From Eq. (39), one can see that $\chi(T)$ in the $T\to 0$ limit has the same temperature dependence as for the Δ_0 phase. The important difference arising from the strong k dependence of the Δ_2 and Δ_3 gaps is reflected in $C_p(T)$, where T^3 behavior is found in the small temperature limit. In

Eq. (38) this dependence is obtained mathematically by the integral variable change $y_i=\beta\cos(\pi x_i)$. The integral limits, after the transformation becomes $(-\beta,+\beta)$ which in the $T\to 0$ limit yield $(-\infty,+\infty)$ (see the Appendix). But in fact, this result is connected to the fact that the gap $\Delta(S_2(k)\pm iS_3(k))$ vanishes in this case on points on the Fermi surface (FS) (see Ref. 26). To show this, we emphasize that for a half-filled band, the FS is given by $\gamma_k=0$. The gap is zero on FS if $S_2(k)=0$ and $S_3(k)+0$. These three relations have point solutions: $k_j^0=\pm\pi/2a$, $j=x,y,z$. Expanding now in the first term of Eq. (19) the $\cos ak_j$ terms from $S_i(k)$, $i=1,2,3$ around k_j^0 up to the first order and changing the integral variables in $y_j=\beta\pi(k_j-k_j^0)$ we reobtain, in the $T\to 0$ limit, the relation given in Eq. (38).

We present another solution for the Δ_2, Δ_3 phase. The two coupled integral equations mentioned at the beginning of Sec. V B also give two real and symmetrical solutions with the same free energy, which is however, greater than the free energy of the $\Delta(S_2(k)\pm iS_3(k))$ phase. We illustrate these solutions with the numerical result of Δ_2, Δ_3, versus T, for the $g_2/t=1.41$ value [Figs. 4(c) and (d)]. In this case, the gaps in the $T\to 0$ limit can be given in a condensed form, as

$$\Delta_2^2(T)+\Delta_3^2(T)=\Delta_2^2(T=0)+\Delta_3^2(T=0)-2T^4[I_{r1}^{2,3}(\Delta_2^2(T=0)+\Delta_3^2(T=0))+2I_{r2}^{2,3}\Delta_2(T=0)\Delta_3(T=0)+O(T^8)\ . \tag{40}$$

In the vicinity of T_{N2}, we obtain

$$\Delta_2^2+\Delta_3^2=t^2(k_{2r}I_0^0(T_{N2},S_2^2/\sqrt{2}))(1-T/T_{N2})\ , \tag{41}$$

where $k_{2r}=2k_{2c}$. $C_p(T)$ and $\chi(T)$ have the same expressions as in Eqs. (38) and (39), in which $I_{ci}^{2,3}$, $i=2,3$ are changed with $I_{ri}^{2,3}$ $i=2,3$. The $T_{N2}/\Delta_i(T=0)$, $i=2,3$ ratio is almost the same for a great variation domain of g_2 and it is close to 3.03 and 1.92 for higher and lower gap solutions, respectively.

The recent neutron diffraction measurements[11] show that the magnetic moments on nearest-neighbor U sites in U_2Zn_{17} have antiparallel orientation. This means a strong repulsive interaction between two heavy electron spins situated on adjacent sites, i.e., a large V contribution. This means that the Δ_2, Δ_3 phase has a great chance to emerge in the heavy-fermion systems, because this SDW state appears as a stable one (see Fig. 1) for great V coupling constant value, and give T^2 and T^3 behavior for $\chi(T)$ and $C_p(T)$, respectively, in the $T\to 0$ limit, in agreement with the experimental data.[3,4] It must be mentioned, that the measured $C_p/T\neq 0$ (i.e., γ_0) for $T=0$ value is due to electrons for which the nesting is not accomplished.

C. $\tilde{\Delta}_4$ phase

The three coupled gap equations which characterize this case are given by Eq. (16) with $i=4,5,6$ and $\Delta_i=0$ for all $i=0$, 1, 2, and 3. The equations obtained allow many solutions (real or complex) which appear at the same Néel temperature T_{N4}. The numerical results concerning the T_{N4}-versus-g_4 curve are presented in Fig. 5(a). The analytic expressions for T_{N4} are the following:

$$\begin{aligned} &T_{N4}=t\exp(-12t/g_4), \quad \text{for } t/T\gg 1\ . \\ &T_{N4}=0.10g_4, \quad \text{for } t/T\sim 1\ . \\ &T_{N4}=g_4/8 \quad \text{for } t/T\ll 1\ . \end{aligned} \tag{42}$$

At this stage, we must mention that T_{Ni}—for all the three analyzed SDW phases in the great coupling constant limit $g^i/t\gg 1$—can be expressed in the following condensed form:

$$T_{Ni}=g^i/4\ , \tag{43}$$

where $g^i=g_0$, $6g_2$, and $g_4/2$ for $i=0$, $i=2$, and $i=4$ phases, respectively. This is an interesting result, which is also illustrated by the numerical data in Figs. 3(b), 4(a), and 5(a).

Some of the possible $\tilde{\Delta}_4$ solutions are presented in Fig. 5(b) together with their energy ($\delta E=E-E_0$) at $T=0$ in function of g_4. The relative positions of the curves remain

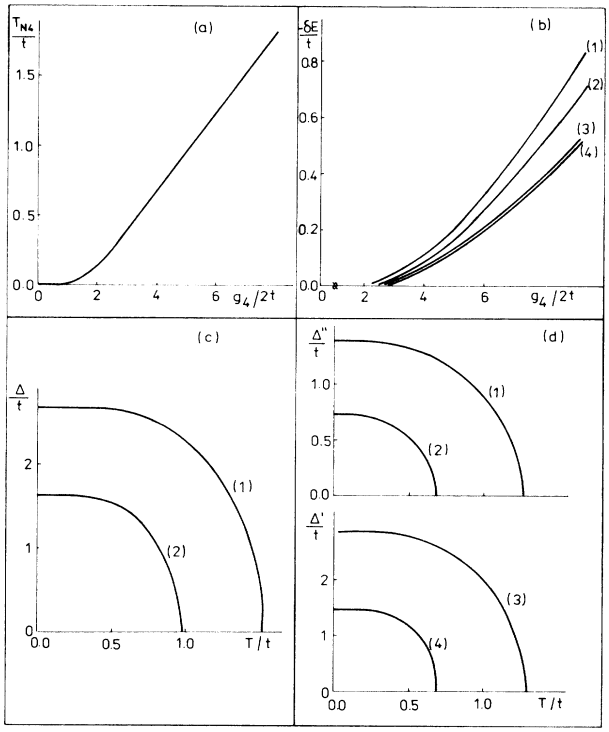

FIG. 5. Characteristics of the Δ_4 phase. (a) The critical temperature vs the coupling constant g_4; (b) some possible solutions for the $\tilde{\Delta}_4$ phase together with their ground-state energy, compared to the energy of the paramagnetic phase $\delta E=E-E_0$ (see text); (c) the reduced gap Δ/t as a function of the reduced temperature T/t for $g_4/t=14$, curve (1) and $g_4/t=10$, curve (2); the reduced gaps Δ''/t and Δ'/t as a function of the reduced temperature T/t for $g_4/t=12$, curve (1), $g_4/t=8$, curve (2), $g_4/t=12$, curve (3), and $g_4/t=8$, curve (4).

the same for $T\neq 0$, too. The lowest free energy for the $\tilde{\Delta}_4$ state could be given by a solution of the form: $|\Delta_S|^2=\Delta^2(\sin^2 ak_x+\sin^2 ak_y+\sin^2 ak_z)$. But such a solution cannot be obtained. Under these conditions, the lowest free energy is given by the solution: $|\Delta_S|^2=\Delta^2(\sin^2 ak_x+\sin^2 ak_y)$ [see curve (1) in Fig. 5(b)]. This solution is a complex one and has the form $\tilde{\Delta}_4^0=\Delta(\sin ak_x\pm i\sin ak_y)$, or an equivalent one. This gap was used for the construction of the phase diagram. In the free energy scale the $\tilde{\Delta}'=\Delta'\sin ak_x$ solution follows [curve (2) in Fig. 5(b)], followed by solutions such as $\Delta''=\Delta_x=\Delta_y=\Delta_z$ [curve (3) in Fig. 5(b)] or $\Delta'''=\Delta_x=\Delta_y$ with $\Delta_z=0$ [curve (4) in Fig. 5(b)]. What is important for the $\tilde{\Delta}_4$ state, is that it has the same symmetry properties as the other $i\geq 1$ SDW states, from the point of view of the $k\rightarrow k+Q$ transformation (this is relevant for the SDW and not $k\rightarrow -k$ as in the superconducting case).

Now we study the above mentioned $\tilde{\Delta}_4^0$ complex solution. In Fig. 5(c) we present the exact numerical results concerning the Δ-versus-T variations at fixed g_4 values. The $\Delta(T=0)/T_{N4}$ ratio is close to 1.6 for small g_4/t values and it slightly increases with the coupling constant. For example, if $g_4/2t=8$, we have $\Delta(T=0)/T_{N4}=1.78$. In the small temperature regime, $\Delta(T)$ can be analytically approximated by

$$\Delta(T)=\Delta(T=0)-g_4T^4\Delta(T=0)I_{c1}^4 \ . \tag{44}$$

Equation (44) is obtained by expanding the $\tanh x$ function and by changing the integral variables in $x_1=\beta(\cos\pi x+\cos\pi y+\cos\pi z)$, $x_2=\beta\sin\pi x$ and $x_3=\beta\sin\pi y$. In the vicinity of T_{N4}, Δ can be expressed as

$$\Delta=t\,[k_{4c}I_0^0(T_{N4},(S_4^2+S_5^2)/\sqrt{2})]^{-1/2}(1-T/T_{N4})^{1/2} \ , \tag{45}$$

where

$$\begin{aligned} &k_{4c}=3t/T_{N4} \quad \text{for } t/T\gg 1 \ , \\ &k_{4c}=2.55 \quad \text{for } t/T\sim 1 \ , \\ &k_{4c}=2 \quad \text{for } t/T\ll 1 \ . \end{aligned} \tag{46}$$

For the specific heat we used the same integral variable transformation as for Eq. (44), obtaining in the $T\rightarrow 0$ limit

$$C_p(T)=T^3I_{c2}^4 \ . \tag{47}$$

With the same technique, the $Y(T)$ function from $\chi(T)$, in the $T\rightarrow 0$ case is

$$Y(T)=T^2I_{c3}^4 \ . \tag{48}$$

As Eqs. (47) and (48) show, the $\tilde{\Delta}_4^0$ solution gives a T^2 dependence in $\chi(T)$ and a T^3 behavior in $C_p(T)$, in the $T\rightarrow 0$ limit. As in the case of the Δ_2, Δ_3 phase these results are connected to the fact that the $\tilde{\Delta}_4^0$ gap vanishes in points on the FS. In this case the three equations which determines the gap zeros on FS are: $\gamma_k=0$, $S_4(k)=0$, and $S_5(k)=0$. The k_j^0 becomes: $k_x^0=0$, $k_y^0=\pm\pi/a$, and $k_z^0=\pm\pi/2a$; or $k_x^0=\pm\pi/a$, $k_y^0=0$, and $k_z^0=\pm\pi/2a$. Thus, from the $\chi(T)$ and $C_p(T)$ point of view, the $\tilde{\Delta}_4^0$ solution also could describe the measured data. But (see Figs. 1 and 2) this phase is strongly connected to the I value and the experimental information obtained up to now suggest a small I contribution, which does not allow us to obtain a stable $\tilde{\Delta}_4$ solution. In future measurements we shall have to analyze the $\Delta(T=0)/T_{Ni}$ values too, since they could offer useful information about the concrete existing SDW phase. Furthermore, we analyze a metastable $\tilde{\Delta}_4$ phase, namely the $\Delta''=\Delta_x=\Delta_y=\Delta_z$ symmetrical and real solution. We present this phase, because of its interesting properties.

The numerical results concerning the Δ''/t-versus-T/t dependence for fixed g_4/t values are presented in Fig. 5(d), curves (1) and (2). The $\Delta''(T=0)/T_{N4}$ ratio in this case is close to one for small g_4/t values and it slightly increases with the coupling constant. For example, if $g_4/t=8$ we have $\Delta''(T=0)/T_{N4}=1.14$. In the small temperature regime the gap can be approximated by

$$\Delta''(T)=\Delta''(T=0)-\tfrac{2}{3}g_4T^3\Delta''(T=0)I_{r1}^4 \ . \tag{49}$$

In this case, the integral I_{r1}^4 is obtained in a different way. We introduce new integral variables as $x_1=\beta(\cos\pi x+\cos\pi y+\cos\pi z)$, $x_2=\beta(\sin\pi x+\sin\pi y+\sin\pi z)$, and $x_3=z$. The integration domain, after some algebra, is transformed to domain D given by

$$(x_1-\beta\cos\pi x_3)^2+(x_2-\beta\cos\pi x_3)^2=4\beta^2 \ .$$

For $T\rightarrow 0$, D passes over the whole (x_1,x_2) plane. The temperature dependence is then obtained directly from the coefficient of the I_{r1}^4 term. The gap expression, for the $T\rightarrow T_{N4}$ is

$$\Delta''=t\,[k_{4r}I_0^0(T_{N4},(S_4+S_5+S_6)^2/\sqrt{3})]^{-1/2}\times(1-T/T_{N4})^{1/2} \ , \tag{50}$$

where $k_{4r}=k_{4c}$ and the S_i terms used in Eqs. (45) and (50) are given in Eq. (15). The specific heat and the magnetic susceptibility for $T\rightarrow 0$ are found using the same procedure as for the I_{r1}^4 term:

$$C_p(T)=T^2I_{r2}^4 \ , \tag{51}$$

and

$$Y(T)=TI_{r3}^4 \ . \tag{52}$$

As it can be seen, an unusual temperature behavior is found at low temperatures, for the physical quantities: $\chi(T)$ depends on T and $C_p(T)$ behaves as T^2 for $T\rightarrow 0$. All these results are due to the specific k dependence of the gap function: Δ'' vanishes on lines on the FS. In this case, besides the $\gamma_k=0$ relation which gives the FS, we have only the $S_4(k)+S_5(k)+S_6(k)=0$ equality, which determines the zeros of the gap on FS. If we fix the k_z value, the two relations mentioned above give point solutions for k_x and k_y, but a continuous variation of the solutions is obtained with k_z used as a parameter which moves on the FS. Thus, the gap vanishes on lines on the FS and this property (in agreement with other results[26]) gives the obtained dependences for the physical quantities in the $T\rightarrow 0$ limit.

In Fig. 5(d), comparatively, we present another temperature dependence of another metastable $\tilde{\Delta}_4$ solution,

namely the Δ'/t-versus-T/t curve, which describes the $\tilde{\Delta}'=\Delta'\sin ak_x$ gap. We mention that this gap also vanishes on lines on the FS.

Unfortunately, the metastable $\tilde{\Delta}_4$ states, like Δ' or Δ'', have greater free energy than the stable $\tilde{\Delta}_4^0$ phase and thus the existence of the $\tilde{\Delta}_4$ solutions which vanishes on lines on the FS is less probable.

VI. DISCUSSION AND CONCLUSIONS

Many experimental data obtained in the last few years prove the existence of an itinerant antiferromagnetic state in heavy-fermion (HF) materials. Our analysis models this phase in the HF systems by a spin-density wave (SDW), the characteristics and properties of which are analyzed in detail in this work. For this purpose, we start from the idea that the same f electrons which give the HF properties also give rise to the SDW characteristics. The used Hamiltonian is based on a simple description of the Kondo lattice systems.[18,19] In this Hamiltonian we introduced new terms (V,J,I) which emphasize the differences between the contributions which arise from different spin configurations on nearest-neighbor sites. Contrary to the classical SDW phase,[14,15] in this case of HF materials, the use of the explicit band structure is of great importance. For this reason we present our analysis in the case of a simple crystal structure. However, the results can be easily generalized to other symmetry species (see Ref. 13).

The description presented herein represents a model in which the exchange and the phononic contributions are equally important. It emphasizes that the competition between the same interactions give rise to superconductivity or SDW properties in the HF systems, and in the two mentioned cases, only the strength of the contributing interactions is different.

After we study the nesting properties, we define the SDW gaps and deduce the characteristic Green's functions of the model. Making use of these, we analyze the gap equations, the phase diagram of the system, the energetical stability, the specific heat $C_p(T)$ and the magnetic susceptibility $\chi(T)$ of different SDW phases. Our study emphasizes that the possible SDW states reflect the symmetry of the crystal lattice. Besides the Δ_0 solution which shows some similarities with the classical Overhauser-type[14] or Fedders-Martin-type[15] phases, two other new stable SDW phases can appear which have k-dependent order parameters (as the experimental data suggested[16,17]). The magnetic phases which we describes are commensurate with the lattice (in agreement with the measurements[11]). They are characterized by a well-defined Q vector which is given by the nesting property. The experimental data show that only a fraction of the Fermi surface is opened by the SDW gaps,[4,16,17] because only a fraction of the band satisfies the nesting conditions in the measured materials. The recent neutron diffraction measurements[11] show a strong V coupling constant (and a weak I contribution) which give rise to a stable Δ_2, Δ_3 phase and which explains the T^2 dependence in $\chi(T)$ and a T^3 behavior in $C_p(T)$ in the $T\to 0$ limit. All these data emphasize upon the fact that the Δ_2, Δ_3 SDW phase has a great chance to describe the magnetically ordered ground state of the HF systems. We mention that the deduced behavior for $C_p(T)$ and $\chi(T)$ is connected to the fact that, for the Δ_2, Δ_3 phase, the gap vanishes on points on the Fermi surface.

In the theoretical description to come, one must consider the SDW and the superconducting phases together. This is claimed by recent experimental data[27] which suggests the coexistence of the two mentioned states. The study of this coexistence is in course of development.

ACKNOWLEDGMENTS

The authors would like to acknowledge the hospitality of the Central Research Institute for Physics, Budapest, of the Wroclaw University, and of the Institute of Physics of Katowice, where parts of this material were presented and discussed.

APPENDIX: INTEGRALS APPEARING IN SEC. V

$$I_0^0(x,y)=\int_0^1 dx_1\int_0^1 dx_2\int_0^1 dx_3 y^2\left[\frac{x}{\epsilon^3}\tanh\frac{\epsilon}{2x}-\frac{1}{2\epsilon^2}\cosh^{-2}\frac{\epsilon}{2x}\right],$$

$$I_1^0=(1/\pi^3)\int_{-\infty}^{+\infty} dx_1\int_{-\infty}^{+\infty} dx_2\int_{-\infty}^{+\infty} dx_3\exp[-2t^2(x_1+x_2+x_3)^2/\Delta_0(T=0)]\ .$$

$$I_2^0=(1/2\pi^3)\int_{-\infty}^{+\infty} dx_1\int_{-\infty}^{+\infty} dx_2\int_{-\infty}^{+\infty} dx_3\int_0^{+\infty} dx_4\left[\cosh^{-2}(t\mid x_1+x_2+x_3\mid)-\frac{x_4}{E_0}\frac{\tanh(E_0/2)}{\cosh(E_0/2)}\right],$$

where $\epsilon=2t(\cos\pi x_1+\cos\pi x_2+\cos\pi x_3)$. We used the notation $E_0^2=4t^2(x_1+x_2+x_3)^2+x_4^2$:

$$I_{c1}^{2,3}=(1/\pi^3)\int_{-\infty}^{+\infty} dx_1\int_{-\infty}^{+\infty} dx_2\int_{-\infty}^{+\infty} dx_3\{[\exp(-E_{2,3;c})][(6(x_1-x_2)^2+2(x_1+x_2-2x_3)^2]/E_{2,3;c}\}$$

$$I_{c2}^{2,3}=(1/\pi^3)\int_{-\infty}^{+\infty} dx_1\int_{-\infty}^{+\infty} dx_2\int_{-\infty}^{+\infty} dx_3 E_{2,3;c}^2\cosh^{-2}(E_{2,3;c}/2)\ ,$$

$$I_{c3}^{2,3}=(1/2\pi^3)\int_{-\infty}^{+\infty} dx_1\int_{-\infty}^{+\infty} dx_2\int_{-\infty}^{+\infty} dx_3\cosh^{-2}(E_{2,3;c}/2)\ ,$$

$$I_{r1}^{2,3}=(1/\pi^3)\int_{-\infty}^{+\infty} dx_1\int_{-\infty}^{+\infty} dx_2\int_{-\infty}^{+\infty} dx_3[\exp(-E_{2,3;r})][(x_1-x_2)^2/E_{2,3;r}]\ ,$$

$$I_{r2}^{2,3}=(1/\pi^3)\int_{-\infty}^{+\infty} dx_1\int_{-\infty}^{+\infty} dx_2\int_{-\infty}^{+\infty} dx_3[\exp(-E_{2,3;r})][(x_1-x_2)(x_1+x_2-2x_3)/E_{2,3;r}]\ ,$$

$$I_{r3}^{2,3}=(1/\pi^3)\int_{-\infty}^{+\infty}dx_1\int_{-\infty}^{+\infty}dx_2\int_{-\infty}^{+\infty}dx_3 E_{2,3;r}^2\cosh^{-2}(E_{2,3;r}/2)\ ,$$

$$I_{r4}^{2,3}=(1/2\pi^3)\int_{-\infty}^{+\infty}dx_1\int_{-\infty}^{+\infty}dx_2\int_{-\infty}^{+\infty}dx_3\cosh^{-2}(E_{2,3;r}/2)\ ,$$

where

$$E_{2,3;c}^2=4t^2(x_1+x_2+x_3)^2+\Delta^2(T=0)[6(x_1-x_2)^2+2(x_1+x_2-2x_3)^2]$$

and

$$E_{2,3;r}^2=4t^2(x_1+x_2+x_3)^2+[\sqrt{6}\Delta_2(T=0)(x_1-x_2)+\sqrt{2}\Delta_3(T=0)(x_1+x_2-2x_3)]^2\ .$$

Also,

$$I_{c1}^4=(1/\pi^3)\int_{-\infty}^{+\infty}dx_1\int_0^{+\infty}dx_2\int_0^{+\infty}dx_3[\exp(-E_{4;c})][(x_2^2+x_3^2)/E_{4;c}]\ ,$$

$$I_{c2}^4=(1/\pi^3)\int_{-\infty}^{+\infty}dx_1\int_0^{+\infty}dx_2\int_0^{+\infty}dx_3 E_{4;c}^2\cosh^{-2}(E_{4;c}/2)\ ,$$

$$I_{c3}^4=(1/\pi^3)\int_{-\infty}^{+\infty}dx_1\int_0^{+\infty}dx_2\int_0^{+\infty}dx_3\cosh^{-2}(E_{4;c}/2)\ ,$$

$$I_{r1}^4=(8/\sqrt{3}\pi^2)\int_{-\infty}^{+\infty}dx_1\int_{-\infty}^{+\infty}dx_2[\exp(-E_{4;r})](x_2^2/E_{4;r})\ ,$$

$$I_{r2}^4=(4/\sqrt{3}\pi^2)\int_{-\infty}^{+\infty}dx_1\int_{-\infty}^{+\infty}dx_2 E_{4;r}^2\cosh^{-2}(E_{4;r}/2)\ ,$$

$$I_{r3}^4=(4/\sqrt{3}\pi^2)\int_{-\infty}^{+\infty}dx_1\int_{-\infty}^{+\infty}dx_2\cosh^{-2}(E_{4;r}/2)\ ,$$

where

$$E_{4c}^2=4t^2x_1^2+\Delta^2(T=0)(x_2^2+x_3^2)$$

and

$$E_{4;r}^2=4t^2x_1^2+x_2^2(\Delta''(T=0))^2\ .$$

---

[1]For a review, see G. R. Stewart, Rev. Mod. Phys. **56**, 755 (1984).

[2]For a recent review of the heavy-fermion theories, see P. A. Lee, T. M. Rice, J. W. Serene, L. J. Sham, and J. W. Wilkins (unpublished).

[3]For a recent review of the experimental status in heavy-fermion systems, see Z. Fisk, H. R. Ott, T. M. Rice, and J. L. Smith (unpublished); Nature **320**, 124 (1986).

[4]H. R. Ott, H. Rudigier, P. Delsing, and Z. Fisk, Phys. Rev. Lett. **52**, 1551 (1984).

[5]Z. Fisk, G. R. Stewart, J. O. Willis, H. R. Ott, and F. Hulliger, Phys. Rev. B **30**, 6360 (1984).

[6]G. R. Stewart, Z. Fisk, J. L. Smith, J. O. Willis, and M. S. Wire, Phys. Rev. B **30**, 1249 (1984).

[7]H. R. Ott, H. Rudigier, Z. Fisk, and J. L. Smith, Phys. Rev. B **31**, 1651 (1985).

[8]T. T. M. Palstra, A. A. Menovsky, and J. A. Mydosh (unpublished); T. T. M. Palstra, A. A. Menovsky, J. van der Berg, A. J. Dirkmaat, P. H. Kes, G. J. Nieuwenhuys, and J. A. Mydosh, Phys. Rev. Lett. **55**, 2727 (1985); F. R. de Boer, J. J. M. Franse, E. Louis, A. A. Menovsky, J. A. Mydosh, T. T. M. Plastra, U. Rauchschwalbe, W. Schlabitz, F. Steglich, and A. de Visser (unpublished).

[9]H. R. Ott, H. Rudigier, E. Felder, Z. Fisk, and B. Batlog (unpublished).

[10]M. R. Norman and D. D. Koelling, Phys. Rev. B **33**, 3803 (1986).

[11]S. M. Shapiro, preprint; D. E. Cox, G. Shirane, S. M. Shapiro, G. Aeppli, Z. Fisk, J. L. Smith, J. Kjems, and H. R. Ott (unpublished); Phys. Rev. B **33**, 3614 (1986).

[12]For some recent approaches not included in Ref. 2, see G. Czycholl and S. Doniach, J. Magn. Magn. Mater. **47&48**, 17 (1985); A. W. Overhauser and J. Appel, Phys. Rev. B **31**, 193 (1985).

[13]M. Gulácsi and Zs. Gulácsi, Phys. Rev. B (to be published). Zs. Gulácsi and M. Gulácsi (unpublished) (see Acknowledgments).

[14]A. W. Overhauser, Phys. Rev. **128**, 1437 (1966).

[15]P. A. Fedders and P. C. Martin, Phys. Rev. **143**, 245 (1966).

[16]H. R. Ott, Physica **130B**, 163 (1985).

[17]H. R. Ott, H. Rudigier, Z. Fisk, and J. L. Smith, J. Appl. Phys. **57**, 3044 (1985).

[18]H. Jichu, T. Matsuura, and Y. Kuroda, Prog. Theor. Phys. **72**, 366 (1984); T. Matsuura, J. Miyake, H. Jichu, and Y. Kuroda, *ibid.* **72**, 402 (1984); K. Miyake, T. Matsuura, and H. Jichu, *ibid.* **72**, 652 (1984).

[19]K. Miyake, T. Matsuura, H. Jichu, and Y. Nagaoka, Progr. Theor. Phys. **72**, 1063 (1985).

[20]K. Miyake, Proceedings of the Eighth Taniguchi Symposium on Theory of Valence Fluctuation State, 1985 (unpublished).

[21]M. Gulácsi, M. Crisan, and Zs. Gulácsi, J. Magn. Magn. Mater. **39**, 290 (1983).

[22]M. Gulácsi and Zs. Gulácsi, Solid State Commun. **56**, 1059 (1985).

[23]G. P. Meisner, A. L. Giorgi, A. C. Lawson, G. R. Stewart, J. O. Willis, M. S. Wire, and J. L. Smith, Phys. Rev. Lett. **53**, 1829 (1984).

[24]A. J. Leggett, Rev. Mod. Phys. **47**, 331 (1975).

[25]R. Balian and N. R. Werthamer, Phys. Rev. **131**, 1553 (1963).

[26]G. E. Volovik and L. P. Gor'kov, Z. Eksp. Teor. Fiz. **88**, 1412 (1985).

[27]See Refs. 3, 7, 8, and B. Batlog, D. Bishop, B. Golding, C. M. Varma, Z. Fisk, J. L. Smith, and H. R. Ott, Phys. Rev. Lett. **55**, 1319 (1985).